
Since January 2020 Elsevier has created a COVID-19 resource centre with free information in English and Mandarin on the novel coronavirus COVID-19. The COVID-19 resource centre is hosted on Elsevier Connect, the company's public news and information website.

Journal of Proteomics 240 (2021) 104191

Contents lists available at ScienceDirect

Journal of Proteomics

journal homepage: www.elsevier.com/locate/jprot

# Identification of cellular proteins interacting with PEDV M protein through APEX2 labeling

Shijuan Dong [a,b,1], Ruiyang Wang [a,1], Ruisong Yu [a], Bingqing Chen [a,b], Fusheng Si [a,b], Chunfang Xie [a], Zhen Li [a,b,*,2]

[a] Institute of Animal Science and Veterinary Science, Shanghai Key Laboratory of Agricultural Genetics and Breeding, Shanghai Academy of Agricultural Sciences (SAAS), Shanghai, PR China

[b] Shanghai Engineering Research Center of Breeding Pigs, Shanghai Academy of Agricultural Sciences (SAAS), Shanghai, PR China

ARTICLE INFO

*Keywords:*
PEDV
Membrane protein
Cellular proteins
APEX2
Interaction

ABSTRACT

Membrane (M) proteins of coronaviruses are the most abundant component of the virus envelope and play crucial roles in virus assembly, virus budding and the regulation of host immunity. To understand more about these functions in the context of PEDV M protein, forty host cell proteins interacting with the M protein were identified in the present study by exploiting the proximity-labeling enzyme APEX2 (a mutant soybean ascorbate peroxidase). Bioinformatic analysis showed that the identified host cell proteins were related to fifty-four signal pathways and a wide diversity of biological processes. Interaction between M and five of the identified proteins (RIG-I, PPID, NHE-RF1, S100A11, CLDN4) was confirmed by co-immunoprecipitation (Co-IP). In addition, knockdown of PPID and S100A11 genes by siRNA significantly improved virus production, indicating that the proteins encoded by the two genes were interfering with or down-regulating virus replication in infected cells. Identification of the host cell proteins accomplished in this study provides new information about the mechanisms underlying PEDV replication and immune evasion.

*Significance:* PEDV M protein is an essential structural protein implicated in viral infection, replication and assembly although the precise mechanisms underlying these functions remain enigmatic. In this study, we have identified 40 host cell proteins that interact with PEDV M protein using the proximity-labeling enzyme APEX2. Co-immunoprecipitation subsequently confirmed interactions between PEDV M protein and five host cell proteins, two of which (S100A11 and PPID) were involved in down-regulating virus replication in infected cells. This study is significant in that it formulates a strategy to provide new information about the mechanisms relating to the novel functions of PEDV M protein.

## 1. Introduction

Porcine epidemic diarrhea (PED) is a swine disease characterized by vomiting, enteritis and typically severe watery diarrhea, with a high mortality rate in neonatal piglets. The causative agent of the disease, first identified in Europe in 1971, was named porcine epidemic diarrhea virus (PEDV) in 1977 [1]. In China, live or inactivated vaccines have been used to control the disease. However, since 2010, variants of PEDV have emerged, causing more severe epidemics [2,3] and even spreading to countries previously free of the disease [4,5].

PEDV, a member of the genus Alphacoronavirus, is an enveloped virus possessing a single-stranded positive-sense RNA genome. The genome is approximately 28 kb, encoding at least seven open reading frames (ORFs): ORF1a, ORF1b, S, ORF3, E, M and N. ORF1a and ORF1b are located downstream of the 5′ untranslated region (UTR) which encodes the virus replicase polyproteins 1a and 1ab. The remaining ORFs at the 3′ end encode four structural proteins [spike (S) protein, membrane (M) protein, envelope (E) protein, nucleocapsid (N) protein], and one accessory protein ORF3 [6,7]. M and E proteins are essential for virus particle assembly and constitute the main part of the virus

* Corresponding author at: Institute of Animal Science and Veterinary Science, Shanghai Key Laboratory of Agricultural Genetics and Breeding, Shanghai Academy of Agricultural Sciences (SAAS), Shanghai, PR China.
*E-mail address:* zhenli60@163.com (Z. Li).

[1] These authors contributed equally to this work.

[2] Mailing address: Institute of Animal Husbandry and Veterinary Science, Shanghai Academy of Agricultural Sciences, Shanghai 201106, China.

https://doi.org/10.1016/j.jprot.2021.104191
Received 16 November 2020; Received in revised form 12 March 2021; Accepted 17 March 2021
Available online 20 March 2021

envelope. The S protein is also a component of the virus envelope and is responsible for receptor binding and virus entry into the host cells. N protein contributes, together with the viral genome RNA, to the formation of a helical nucleocapsid. ORF3 protein, which is probably a nonstructural protein with ion channel activity, enhances the proliferation of the virus and inhibits cell apoptosis [8,9].

In addition to a role in virus assembly, PEDV M protein also modulates the host immune response by inducing neutralizing antibodies in the presence of complement [10], or by inhibiting IFN-β and interferon regulatory Factor 3 (IRF3) promoter activities [11]. In cultured swine intestinal epithelial cells, PEDV M protein induced cell cycle arrest at the S-phase via the cyclin A pathway [12]. However, although several key functions of PEDV M protein have now been identified, the underlying mechanisms involved are less well understood.

In recent years, in addition to co-precipitation, proximity labeling strategies have been adopted to uncover weak and transient protein-protein interactions [13]. One of techniques uses a modified or a chimeric soybean peroxidase (APEX) to biotinylate proximate proteins in living cells [14,15]. APEX2 catalyzes the oxidation of biotin-phenol in the presence of $H_2O_2$ to generate a short-lived (<1 ms) biotin-phenoxyl radical that tags proteins proximal to APEX2 [15]. Biotin tagged proteins are then enriched using streptavidin beads and identified by mass spectrometry. In order to better understand the workings of PEDV M, we have now applied the APEX labeling method to identify interacting host cell proteins.

## 2. Materials and methods

### 2.1. Cells and virus

IPEC-J2 and Hela cells were cultured in Dulbecco's Modified Eagle Medium (DMEM) (Gibco BRL, Gaithersburg, MD, USA) supplemented with 10% fetal bovine serum (FBS) (Gibco BRL, Gaithersburg, MD, USA), 100 U/mL penicillin and 100 μg/mL streptomycin at 37 °C and in a 5% $CO_2$-enriched atmosphere. The cell culture-adapted PEDV DR13$^{att}$ strain (JQ023162; isolated from a commercial vaccine of Green Cross, South Korea) was propagated and titrated into Vero cells with DMEM supplemented with 2% FBS.

### 2.2. Creation of plasmids in this study

M, peptidyl-prolyl cis-trans isomerase D (PPID), claudin (CLDN4), retinoic acid-inducible gene I (RIG-I), S100A11, Na(+)/H(+) exchange regulatory cofactor NHE-RF1 (NHE-RF1) and cyclin-dependent kinase-like 2 (CDKL2) expression plasmids containing tags were generated using the homologous recombinant method. M-HA gene was amplified by RT-PCR using PEDV DR13$^{att}$ (JQ023162) RNA as template and cloned into vector pCAGGS-HA with homologous recombinant reagent (one step cloning kit, Vazyme, China) to construct the recombinant plasmid pCAGGS-M-HA. PPID/CLDN4/RIG-I/S100A11/NHE-RF1/CDKL2-Flag genes were amplified by RT-PCR using full-genome RNA of Vero cells as template and cloned into vector pCAGGS using the homologous recombination kit, and the recombinant plasmids pCAGGS-PPID/CLDN4/RIG-I/S100A11/NHE-RF1/CDKL2-Flag were constructed. All the plasmids were verified by sequencing.

### 2.3. Creation of M-linker-APEX2-HA constructs

pcDNA3.0 APEX2-NES (plasmid#49386) [15] was purchased from Addgene. To generate M-linker-APEX2-HA fusion constructs, M-linker and Linker-APEX2-HA fragments were amplified by PCR using PEDV DR13$^{att}$ (JQ023162) RNA and pcDNA3.0 APEX2-NES, respectively as templates. M-linker and Linker-APEX2-HA fragments were then cloned into vector pCI-neo, previously linearized using restriction enzymes *Eco*RI and *Xba*I, using a homologous recombination kit to create the M-linker-APEX2-HA construct. APEX2-HA was amplified by PCR using pcDNA3.0 APEX2-NES as template and cloned into linearized vector pCI-neo using a homologous recombination kit to create the APEX2-HA construct. The two constructs were confirmed by sequencing.

### 2.4. Detecting the expression of M-linker-APEX2-HA protein

IPEC-J2 cells seeded in a 10-cm diameter culture dish (Corning) were transfected with plasmids expressing M-linker-APEX2-HA and APEX2-HA using lipofectamine 2000 according to the manufacturer's instructions. Transfected cells were harvested at 48 h post-transfection (hpt) and lysed in 60 μL lysis buffer containing protease inhibitor cocktail. Samples were subjected to western blot with anti-HA protein mAb. Expression experiments were repeated three times to confirm reproducibility (see Replicates 1–3 in Fig. 1).

### 2.5. Affinity capture of biotinylated proteins by APEX2-labeling

IPEC-J2 cells in 10-cm dishes were transfected with plasmids expressing M-linker-APEX2-HA and APEX2-HA using lipofectamine 2000. Biotin-phenol labeling assays were performed according to previously published protocols [15]. Briefly, after 48 hpt, cells were incubated in the presence of 0.5 mM biotin-phenol for 30 min, after which hydrogen peroxide ($H_2O_2$) was added to a final concentration of 1 mM. The dishes were then gently agitated for 1 min to ensure equal distribution. The reaction was then quenched and the cells were washed three times by removing the suspension liquid and replacing with quench solution (5 mM Trolox, 10 mM sodium ascorbate and 10 mM sodium azide in DPBS). Cells were then lysed in 60 μL lysis buffer containing a protease inhibitor cocktail and PMSF. Residual cells and cell debris adhering to the culture dish were scraped into the lysates which, after 30 min on ice, were centrifuged at 14,000 ×*g* for 10 min at 4 °C. Supernatants were collected and incubated with streptavidin-coated magnetic beads (Pierce, catalog No. 88817) previously washed twice with RIPA buffer. The beads were then washed twice with 1 mL RIPA lysis buffer, once each with 1 mL 1 M KCL, 1 mL 0.1 M $Na_2CO_3$ and 1 mL 2 M urea in 10 mM Tris-HCL, and again twice with 1 mL RIPA lysis buffer. Biotinylated proteins were then eluted by boiling the beads in 80 μL 3× protein loading buffer supplemented with 20 mM dithiothreitol (DTT) and 2 mM biotin, followed by SDS-PAGE and silver staining. Experiments were carried out three times to confirm reproducibility (Replicates 1–3 in Fig. 2 and Supplemental Fig. S1).

### 2.6. LC-MS/MS analysis

Eluted proteins were separated by electrophoresis on 10% gels. For mass spectrometry, pieces of the SDS-PAGE gel were destained with 30% acetonitrile (ACN)/100 mM $NH_4HCO_3$ and dried in a vacuum centrifuge. In-gel proteins were reduced with dithiothreitol (10 mM DTT/100 mM $NH_4HCO_3$) for 30 min at 56 °C and then alkylated with iodoacetamide (200 mM IAA, 100 mM $NH_4HCO_3$) in the dark at room temperature for 30 min. Gel pieces were rinsed sequentially with 100 mM $NH_4HCO_3$ and ACN and digested overnight in a solution of 25 mM $NH_4HCO_3$ containing 12.5 ng/μL trypsin. Peptides were extracted three times with 60% ACN/0.1% TFA and, after pooling, the extracts were dried by vacuum centrifugation. Tryptic peptide samples were injected into a Q Exactive mass spectrometer coupled to Easy nLC (Thermo Fisher Scientific). Peptide mixtures were loaded onto a C18-reversed phase column (length 15 cm, inner diameter 75 μM) packed in-house with RP-C18 5 μM resin in buffer A (0.1% formic acid in HPLC-grade water) and separated with a linear gradient of buffer B (0.1% formic acid in 84% acetonitrile) over 60 min at a flow rate of 250 nL/min controlled by IntelliFlow Technology. MS data was acquired using a data-dependent top10 method dynamically choosing the most abundant precursor ions from the survey scan (300–1800 *m/z*) for HCD fragmentation. Determination of the target value is based on predictive Automatic Gain Control (pAGC). Dynamic exclusion duration was 20 s. Survey scans

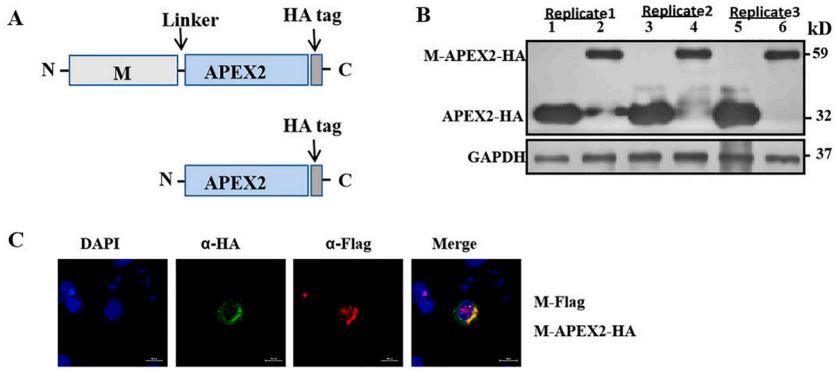


**Fig. 1.** Expression and co-localization of M-Flag and M-APEX2-HA recombinant proteins. (**A**) A schematic drawing of the M-APEX2-HA and APEX2-HA constructs. M gene (light grey) was ligated to 5′ end of APEX2 (blue) with a linker encoding a short peptide (GlyGlySer). HA tag (dark grey) sequence was added to the 3′ end of APEX2 for easy tracking of the recombinant proteins. (**B**) Analysis of recombinant protein expression by M-APEX2-HA and APEX2-HA in IPEC-J2 cells. The expression experiment was repeated three times. (**C**) Co-localization analysis of M-Flag and M-APEX2-HA recombinant proteins. Hela cells were co-transfected with plasmids expressing M-Flag and M-APEX2-HA proteins and the cells were fixed and stained with corresponding anti-HA and anti-Flag mAbs. (For interpretation of the references to colour in this figure legend, the reader is referred to the web version of this article.)

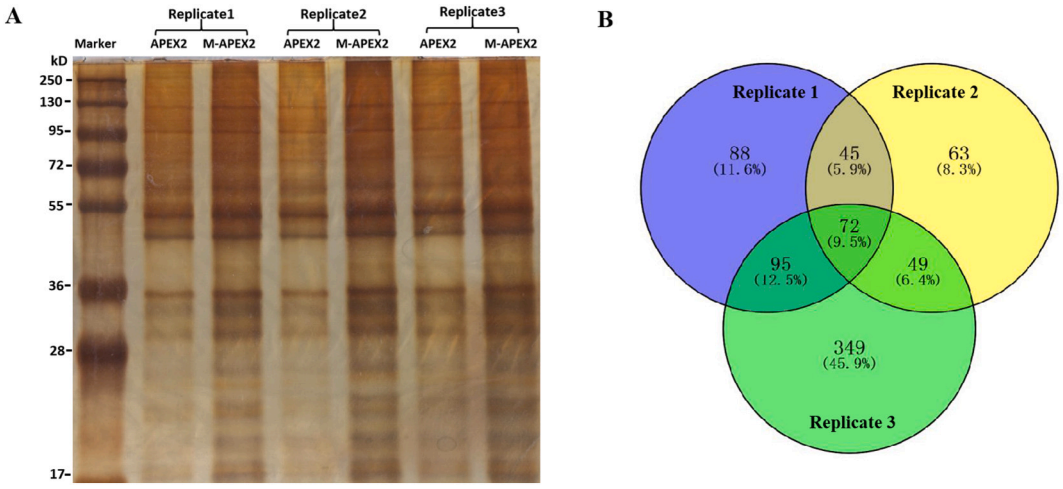


**Fig. 2.** Host cell proteins identified by APEX2-labeling. (**A**) Silver staining of M-APEX2-interacting and APEX2-interacting proteins after SDS-PAGE. Three labeling experiments were conducted with each construct. (**B**) Intersection of identified host cell proteins obtained in three M-APEX2–HA labeling tests. Blue, yellow and green circles and the figures within represent the three replicated tests and the number of host cell interacting proteins identified. (For interpretation of the references to colour in this figure legend, the reader is referred to the web version of this article.)

were acquired at a resolution of 70,000 at *m/z* 200, and resolution for HCD spectra was set to 17,500 at m/z 200. Normalized collision energy was 27 eV and the underfill ratio, which specifies the minimum percentage of the target value likely to be reached at maximum fill time, was defined as 0.1%.

### 2.7. Data analysis

The MS data were analyzed using MaxQuant software version 1.3.0.5. The processed MGF files were searched against the uniprot sus database (50,046 total entries, downloaded 06/07/2018) without specifying enzyme cleavage rules. Carbamidomethylation of cysteines was defined as fixed modification, while protein N-terminal acetylation and methionine oxidation were defined as variable modifications for database searching. Search parameters were set as follows: peptide mass tolerance ±20 ppm, MS/MS tolerance 0.1 Da, maximum missed cleavage 2 (with an allowance for 2 missed cleavages). Variable modification: Oxidation (M). Label-free peptide quantification based on extracted ion chromatograms, and spectral counts and validation, was performed using MaxQuant software. The cutoff of global false discovery rate (FDR) for peptide and protein identification was set to 0.01. Protein abundance was calculated on the basis of the normalized spectral protein intensity (LFQ intensity).The functional annotation and classification of all the cellular proteins identified by M-APEX2-HA were determined using the Gene Ontology (GO) program Blast2GO (https://www.blast2go.com/) and Kyoto Encyclopedia of Genes and Genomes (KEGG) analysis (http://www.genome.jp/kaas-bin/kaas_main).

### 2.8. Co-immunoprecipitation (Co-IP) assay

For analysis of interaction between M-HA and overexpressed cellular target protein, Hela cells seeded into 10-cm diameter culture dishes were co-transfected with the corresponding expression plasmids. Transfected cells were harvested at 36 hpt and lysis buffer containing 1 mM protease inhibitor was added before incubating for 30 min on ice. After centrifugation at 14,000 ×*g* for 10 min, the lysate supernatants containing 1–2 mg of total protein were incubated overnight with mouse mAb against Flag tag with gentle rocking at 4 °C. Protein A/G beads washed with cell lysate were added to supernatants and incubated with gentle rocking for 12 h at 4 °C. Beads were washed four times with cold cell lysate and boiled with 1 × SDS loading buffer for 10 min, followed by SDS-PAGE.

To analyse interactions of PEDV M protein with host cell proteins, Vero cells seeded in 10-cm-diameter culture dishes were infected with PEDV DR13$^{att}$ at a multiplicity of infection (MOI) of 0.1. After 36 h post-infection (hpi), the infected cells were lysed, followed by centrifugation at 14,000 ×*g* for 10 min. Supernatants were precipitated with anti-M protein mAb and incubated with gentle rocking overnight at 4 °C. Protein A/G beads washed with cell lysate were added to supernatant fractions and incubated with gentle rocking for 12 h at 4 °C. The beads were then washed four times with cold cell lysate and boiled with 1 × SDS loading buffer for 10 min, followed by SDS-PAGE.

### 2.9. Western blot analysis

Whole-cell extracts and protein samples were separated by 10% SDS-PAGE and then transferred to PVDF membranes, followed by blocking with 10% nonfat milk in Tris-buffered saline-Tween (TBST) and incubated with the indicated primary antibodies at room temperature for 1 h. After washing with TBST, membranes were incubated with HRP-conjugated goat anti-rabbit IgG or goat anti-mouse IgG at room temperature for 1 h. Specific protein bands were visualized by enhanced chemiluminescence using ECL plus western blot detection reagents (GE Healthcare, Chalfont St Giles, UK) according to the manufacturer's instructions.

### 2.10. Immunofluorescence assay

Hela cells were selectively transfected with the indicated plasmids using lipofectamine 2000 according to the manufacturer's instructions, and fixed with 5% paraformaldehyde at 24 hpt. After permeabilization with Triton X-100, all the cells were incubated with specific primary antibodies followed by incubation with appropriate secondary antibodies. Cells were stained with DAPI and observed with a Zeiss Scope A1 microscope (Zeiss Microsytems, Germany).

### 2.11. RNA interference experiments and viral infectivity

Double-stranded siRNAs targeting PPID, CLDN4, RIG-I, S100A11, NHE-RF1 and a negative control were designed and synthesized by Genepharma Co. (Shanghai, China) (Table 1). Vero cells were transfected with 175 nM PPID, CLDN4, RIG-I, S100A11, NHE-RF1 siRNAs or siRNA negative control, and then infected 16 hpt with PEDV DR13$^{att}$ at an MOI of 1.0. Following incubation at 37 °C for 1 h, the virus inoculum was removed, the cells were washed three times with PBS and subsequently incubated in fresh DMEM. Virus titers in culture supernatants were determined after 18 hpi.

### 2.12. RNA extraction and real time RT-PCR

Total RNA was extracted from cells using the Axygen reagent (Axygen, China) and subjected to reverse transcription with reverse transcription reagent (Promega, USA). qRT-PCR was performed on an ABI 7500-fast Real-time PCR system (ABI, USA). Each 20 μL qPCR reaction mixture contained 2 μL reverse transcription sample, 10 μL Tli RNaseH Plus (2×), 0.4 μL forward and reverse primers (10 μM), 0.4 μL ROX Reference Dye II (50×), and 6.8 μL sterile purified water. Amplification was performed as follows: 95 °C for 30 s, followed by 40 cycles of 95 °C for 5 s and 60 °C for 34 s. Each reaction was performed in triplicate and GAPDH was used as the internal control. qRT-PCR data were analyzed using the 2-$^{\triangle\triangle}$ CT method.

**Table 1**
Sequences of cellular gene siRNAs.

| Gene | | siRNA sequence(5′-3′) |
|---|---|---|
| CLDN4 | Sense | CGCACAGACAAGCCUUACTT |
| | antisense | GUAAGGCUUGUCUGUGCGTT |
| PPID | Sense | GGAGAUAGCACCAGAAGAUTT |
| | antisense | AUCUUCUGGUGCUAUCUCCTT |
| S100A11 | Sense | GGUUAUAACUACACUCUCUTT |
| | antisense | AGAGAGUGUAGUUAUAACCTT |
| NHE-RF1 | Sense | GGCCUCGGCUCUGUACCAUTT |
| | antisense | AUGGUACAGAGCCGAGGCCTT |
| RIG-I | Sense | GCAGAGAAAUUGGUGGAAUTT |
| | antisense | AUUCCACCAAUUUCUCUGCTT |
| Negative control | Sense | UUCUCCGAACGUGUCACGUTT |
| | antisense | ACGUGACACGUUCGGAGAATT |

### 2.13. Statistical analysis

SPSS software (SPSS 11.5 for Windows) was used for statistical analyses (one-way ANOVA). Data are expressed as mean values ± standard error of means (SEM). The *t*-test was employed to determine the statistical significance ($p < 0.05$) of the differences between the means. Data relating to viral RNA copies and virus titers were converted to $\log_{10}$ to maintain a normal distribution.

## 3. Results

### 3.1. Construction of M-APEX2-HA and APEX2-HA and validation of their expression

In order to produce a fusion protein for proximal biotin labeling, the PEDV M gene was linked to APEX2 gene with a nine amino acid linker in the expression vector pCI-neo (Fig. 1A). A fragment of the HA tag was added to the 3′ end of APEX2. Expression plasmid APEX2-HA was used as the mock control. Expression plasmids M-APEX2-HA and APEX2-HA were transfected into IPEC-J2 cells, and the corresponding fusion proteins M-APEX2-HA and APEX2-HA were detected at 48 hpt by western blot (Fig. 1B).

### 3.2. M-APEX2-HA and M-Flag proteins partly co-localized

In order to identify host cell proteins that interact with PEDV M protein, it is essential that the M-APEX2-HA fusion protein takes the same or a similar trafficking route into the cells as the M protein. To confirm this, Hela cells were co-transfected with plasmids expressing M-APEX2-HA and M-Flag proteins and the subcellular localization of the proteins was examined (Fig. 1C). This revealed that M-APEX2-HA fusion protein was partly overlapped with M-Flag fusion protein, indicating that M-APEX2-HA fusion protein shared some host cell-interacting proteins with the M-Flag protein.

### 3.3. Forty biotinylated proteins identified

Constructs of M-APEX2–HA and APEX2-HA were transfected into IPEC-J2 cells and the M protein interacting proteins were biotinylated, purified using streptavidin beads (Fig. 2A) and identified by mass spectrometry (LC-MS/MS). A total of 1419 biotinylated M-APEX2-HA interacting proteins were identified in M-APEX2-HA labeling tests, of which 1055 proteins were recorded in all three tests (Supplemental Fig. S1). After excluding coincident proteins identified in the APEX2-HA labeling tests from these 1419, 761 proteins were obtained as candidate M-interacting proteins, among which 72 proteins were identified at the same time in each of the three individual tests (Fig. 2B). Of these, 40 were annotated with high confidence (Unique Peptide ≥2) (Table 2).

### 3.4. Identified host cell proteins involved in different biological processes and signal pathways

All of the identified 40 proteins were subjected to bioinformatics analysis. Three main types of annotations, i.e. biological processes, cellular components and molecular functions, were obtained from the gene ontology (GO) consortium website (Fig. 3A). The biological processes annotation showed that some proteins were involved in ribonucleoprotein complex assembly, endoplasmic reticulum organization, and regulation of DNA repair (Fig. 3B). Cellular components annotation assigned other proteins to organelle (38%), extracellular exosome (33.0%), cytoplasm (5.0%), and membrane-bounded vesicle (3.0%) categories. Enrichments based on molecular functions annotation were small molecule binding, structural molecule activity, and actin filament binding. Analysis using the KEGG reference pathway database assigned the 40 protein sequences to eight pathways (Fig. 3C), among which three signal pathways were related to immune responses, i.e. Fc gamma

**Table 2**
Putative M-APEX2 protein-interacting host cell proteins identified from MS data.

| Protein name | Gene name | Peptides | Sequence coverage (%) | iBAQ intensity (%) |
|---|---|---|---|---|
| Retinol-binding protein 4 | RBP4 | 5 | 20.1 | 25,396,000 |
| Neutral alpha-glucosidase AB | GANAB | 5 | 5.5 | 2,740,500 |
| Serine/arginine-rich splicing factor 1 | SRSF1 | 4 | 16.5 | 14,908,000 |
| RuvB-like helicase | RUVBL1 | 4 | 7.1 | 3,780,100 |
| Endonuclease domain containing 1 | ENDOD1 | 4 | 8.1 | 4,674,700 |
| Glutathione synthetase | GSS | 4 | 7.2 | 2,870,200 |
| Coactosin like F-actin binding protein 1 | COTL1 | 3 | 18.3 | 10,870,000 |
| Calpain small subunit 1 | CAPNS1 | 3 | 15 | 8,728,000 |
| Proteasome subunit alpha type | PSMA1 | 3 | 9.9 | 8,589,500 |
| Integral membrane protein 2B | ITM2B | 3 | 6 | 1,940,600 |
| Peptidyl-prolyl cis-trans isomerase D | PPID | 3 | 5.8 | 753,450 |
| Retinoic acid-inducible gene 1 protein(RIG-1) | DDX58 | 3 | 2.5 | 945,280 |
| MAP7 domain containing 1 | MAP7D1 | 3 | 2.3 | 292,250 |
| von Willebrand factor A domain containing 8 | VWA8 | 3 | 1.2 | 57,491 |
| 60S acidic ribosomal protein P2 | RPLP2 | 2 | 18 | 8,997,500 |
| Protein S100-A11 | S100A11 | 2 | 13.5 | 49,645,000 |
| Chromatin target of PRMT1 protein | CHTOP | 2 | 10 | 21,170,000 |
| Transmembrane 4 L six family member 1 | TM4SF1 | 2 | 9.4 | 47,944,000 |
| CD99 molecule | CD99L2 | 2 | 11.2 | 10,849,000 |
| Na(+)/H(+) exchange regulatory cofactor NHE-RF | SLC9A3R1 | 2 | 6.4 | 2,093,100 |
| Claudin | CLDN4 | 2 | 8.9 | 3,732,800 |
| Destrin (Actin-depolymerizing factor) | DSTN DSN | 2 | 12.6 | 6,091,100 |
| 40S Ribosomal protein S15 | RPS15 | 2 | 7.8 | 0 |
| Activator of HSP90 ATPase activity 1 | AHSA1 | 2 | 3.9 | 1,175,700 |
| Lectin, mannose binding 1 | LMAN1 | 2 | 6.7 | 2,853,100 |
| Rac family small GTPase 2 | RAC2 | 2 | 7.3 | 0 |
| Epithelial cell adhesion molecule | TACSTD1 | 2 | 6.2 | 4,326,200 |
| Terpene cyclase/mutase family member | LSS | 2 | 2.7 | 782,840 |
| RALY heterogeneous nuclear ribonucleoprotein | RALY | 2 | 4.1 | 703,320 |
| Serine/threonine kinase receptor associated protein | APAF1 | 2 | 5.4 | 1,390,100 |
| Reticulon | RTN3 | 2 | 12.1 | 11,197,000 |
| Thyroid hormone receptor-associated protein 3 | THRAP3 | 2 | 3.3 | 498,110 |
| Isocitrate dehydrogenase [NAD] subunit, mitochondrial | IDH3A | 2 | 4.2 | 1,395,200 |
| Malic enzyme | ME1 | 2 | 3.4 | 723,110 |
| ATPase ASNA1 | ASNA1 | 2 | 3.6 | 1,758,600 |
| 3-Hydroxy-3-methylglutaryl coenzyme A synthase | HMGCS2 | 2 | 3.3 | 1,171,000 |
| Basal cell adhesion molecule | BCAM | 2 | 3.9 | 2,481,800 |
| Prolyl 3-hydroxylase 1 | P3H1 | 2 | 2.5 | 324,770 |
| E3 UFM1-protein ligase 1 | SPATA5 | 2 | 2.1 | 160,110 |
| Ribosome binding protein 1 | RRBP1 | 2 | 0.7 | 0 |

R-mediated phagocytosis, the RIG-I-like receptor signaling pathway and the B cell receptor signaling pathway.

### 3.5. Further validation of interactions between PEDV M protein and five host cell proteins

Co-immunoprecipitation (Co-IP) involving five selected proteins (S100A11, NHE-RF1, CLDN4, RIG-I and PPID) was used to provide additional proof of interaction between the 40 host cell proteins and PEDV M protein. Hela cells were transfected with plasmids expressing M-HA and S100A11/NHE-RF1/CLDN4/RIG-I /PPID-Flag, and Co-IP was performed with anti-Flag mAb to capture protein complexes. CDKL2, shown to interact with APEX2-HA but not M-APEX2-HA, served as the negative control. Probing with anti-HA-mAb detected M protein in the S100A11, NHE-RF1, CLDN4, RIG-I and PPID Co-IP samples but not in CDKL2 (Fig. 4A), thereby confirming that PEDV M protein interacted with these host cell proteins. These interactions were further validated by applying the Co-IP assay to PEDV-infected Vero cells. Separation by SDS-PAGE of IP protein from lysates of PEDV-infected Vero cells and mock-infected cells, and visualization by western blot using anti-S100A11, -NHE-RF1, -CLDN4, -RIG-I, or -PPID rabbit polyclonal antibodies, confirmed that M protein could interact with the five host cell proteins in PEDV-infected cells (Fig. 4B).

### 3.6. Co-localization analysis of M protein and intracellular protein

Extensive cytoplasmic co-localization of M protein with the five validated host cell proteins (S100A11, NHE-RF1, PPID, CLDN4 and RIG-I) was observed when Hela cells were co-transfected with plasmids expressing M-HA and S100A11/NHE-RF1/CLDN4/RIG-I/PPID/CDKL2-Flag proteins (Fig. 5). Pearson's correlation coefficient values (Rr) were 0.780, 0.728, 0.805, 0.954 and 0.928, respectively compared with 0.558 in the case of M protein and CDKL2.

### 3.7. Knockdown of S100A11 and PPID gene expression promoted PEDV production

After first validating siRNA knockdown efficiencies against S100A11, NHE-RF1, CLDN4, RIG-I and PPID genes by real time RT-PCR (Fig. 6A) and western blot (Fig. 6B), we investigated the effects of silencing these genes on PEDV production. Infection tests revealed that virus titers in suspensions of Vero cells with PPID and S100A11 knockdown were significantly higher compared with negative controls (Fig. 6C). However, PEDV proliferation was not significantly affected by knockdown of NHE-RF1, CLDN4 and RIG-I genes.

## 4. Discussion

While it is generally accepted that M proteins of coronaviruses play pivotal roles in virus assembly and replication, the underlying mechanisms involved are still unclear although the mapping of host cell proteins that interact with viral M proteins may provide valuable insights. In the present study, GO analysis identified 40 interacting host cell proteins variously involved in endoplasmic reticulum organization,

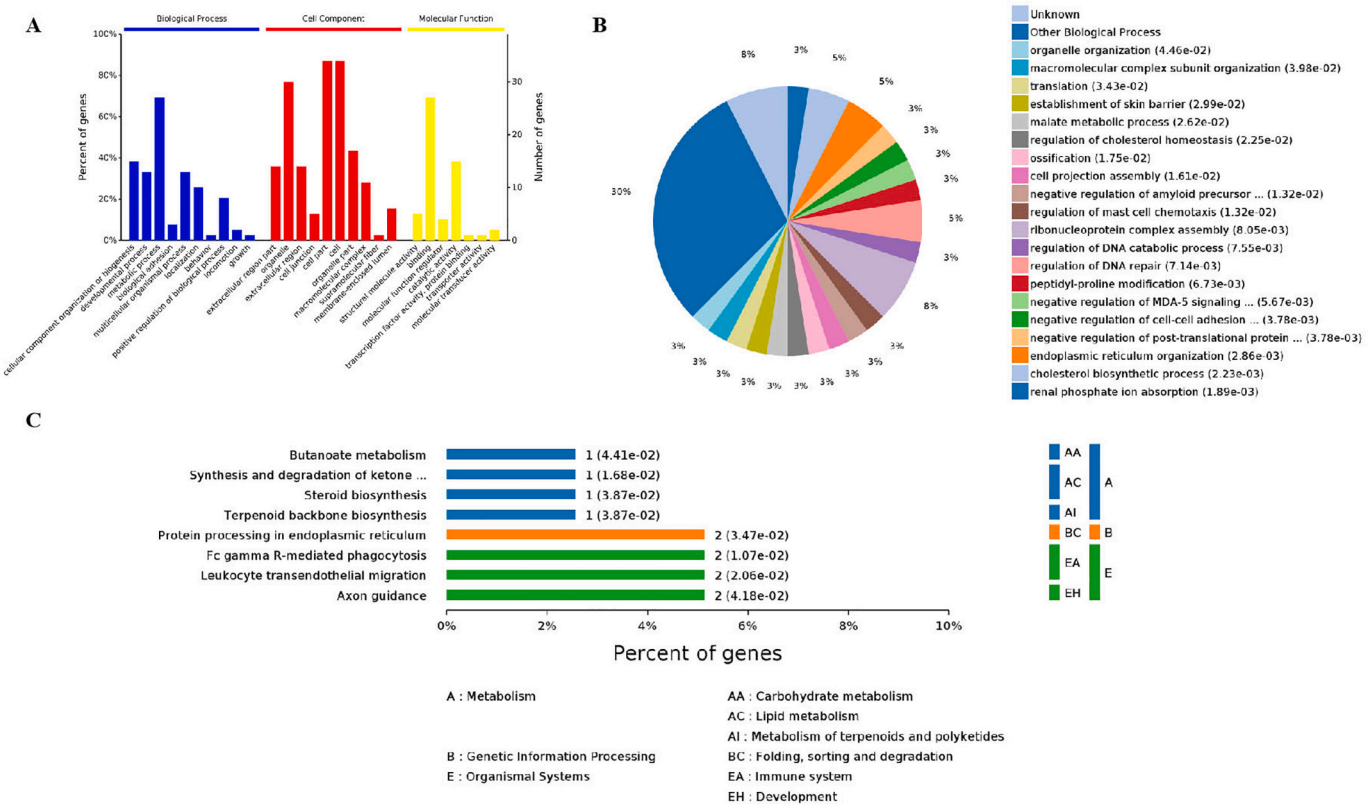


**Fig. 3.** Bioinformatics analysis of host cell proteins putatively identified as interacting with M-APEX2 proteins. (**A**) Annotation of proteins interacting with PEDV M protein using Gene Ontology. (**B**) Molecular function of proteins interacting with PEDV M protein using Gene Ontology. (**C**) KEGG analysis of host cell proteins interacting with PEDV M protein.

negative regulation of cell-cell adhesion, regulation of post-translational protein modification, and negative regulation of the MDA-5 signaling pathway. KEGG pathway analysis showed these 40 proteins to be enriched in 54 signaling pathways relating to immune response (i.e. Ras, B/T cell receptor and TNF signaling pathways), cell cycle and apoptosis. These data should serve to highlight those cellular pathways in which PEDV M protein is involved while fulfilling its functions. Among the 40 proteins, those previously thought likely to impact on virus replication, cell proliferation and the host innate immune response were considered the most plausible candidates influencing PEDV infection. Consequently, S100A11, NHE-RF1, CLDN4, RIG-I and PPID were selected for validation, with S100A11 and PPID found to play negatively regulating roles in PEDV proliferation.

Host immune response-related RIG-I (DDX58 gene) was among the host cell proteins identified as interacting with PEDV M protein, but we have not yet been able to assign a specific function. During viral infection, RIG-I and melanoma differentiation-associated gene 5 (MDA5) act as host pattern recognition receptors (PRRs) that spot double-stranded RNA and then activate downstream signaling of IFNα/β production [16]. It has been reported that coronaviruses have developed various measures to evade innate immunity. Siu and coworkers showed that SARS-CoV M protein interacted with RIG-I, TANK Binding Kinase 1 (TBK1), IKBkinases (IKK), and TNF receptor-associated factor 3 (TRAF3) in the cytoplasm to inhibit type IFN production [17]. Subsequently, they confirmed that the first transmembrane domain (TM1) of SARS-CoV M protein was capable of binding with RIG-I, TANK Binding Kinase 1 (TBK1), IKKε and TRAF3, and prevented the interaction of TRAF3 with its downstream effectors [18]. The interaction between PEDV M protein and RIG-I reported here provides a possible explanation for inhibitory effect of PEDV on RIG-I mediated IFN-β production [19]. Zhang and colleagues reported that PEDV suppressed type IFN production and ISGs expression in Marc-145 cells and identified 10 non-structural and structural proteins including M as the viral IFN antagonists [20]. They confirmed that PEDV nsp1 caused CREB binding protein (CBP) degradation by the proteasome-dependent pathway, but the mechanism through which PEDV M protein inhibited type IFN production was not investigated. However, in the present study, interference of RIG-I expression with siRNA resulted in an insignificant promotion of PEDV proliferation. The interaction between PEDV M protein and RIG-I needs further investigation, and the possibility that this interaction is linked to PEDV M protein inhibition of type IFN production cannot be excluded.

We have also confirmed interaction between PEDV M protein and S100A11, a member of the S100 family of EF-hand $Ca2^{+}$-binding proteins. S100A11 plays a key regulatory role in the diverse cellular processes associated with cancer, including proliferation, apoptosis, cell cycle, migration, invasion, and epithelial-mesenchymal transformation (EMT) [21]. Until now, there have been no reports linking S100A11 to virus proliferation. Our findings show that a decrease in the expression level of S100A11 significantly increased PEDV production compared to negative controls although the underlying mechanism is unclear. S100A11 plays a role in the contact inhibition of cell growth. When normal human fibroblasts reached confluence, S100A11 was phosphorylated and transported into nuclei where it inhibited DNA synthesis [22]. Knockdown of S100A11 may lead to increased cell proliferation, thereby promoting PEDV production [9].

PPID, also named CyP40, another host cell protein identified as interacting with M protein, is a member of the peptidyl-prolyl cis-trans isomerase (PPIase) family. As far as we are aware, this is the first time that PPID has been shown to interact with a coronavirus structural protein. SARS-CoV non-structural protein (NSP1) interacts with a group of host proteins belonging to the PPIase family (PPIA, PPIB, PPIH, PPIG, FKBP1A, FKBP1B) and plays an important role in immune cell activation [23]. PPID contributes to protein folding, ligand binding and nuclear sorting of glucocorticoid, estrogen and progesterone receptors [24–26].

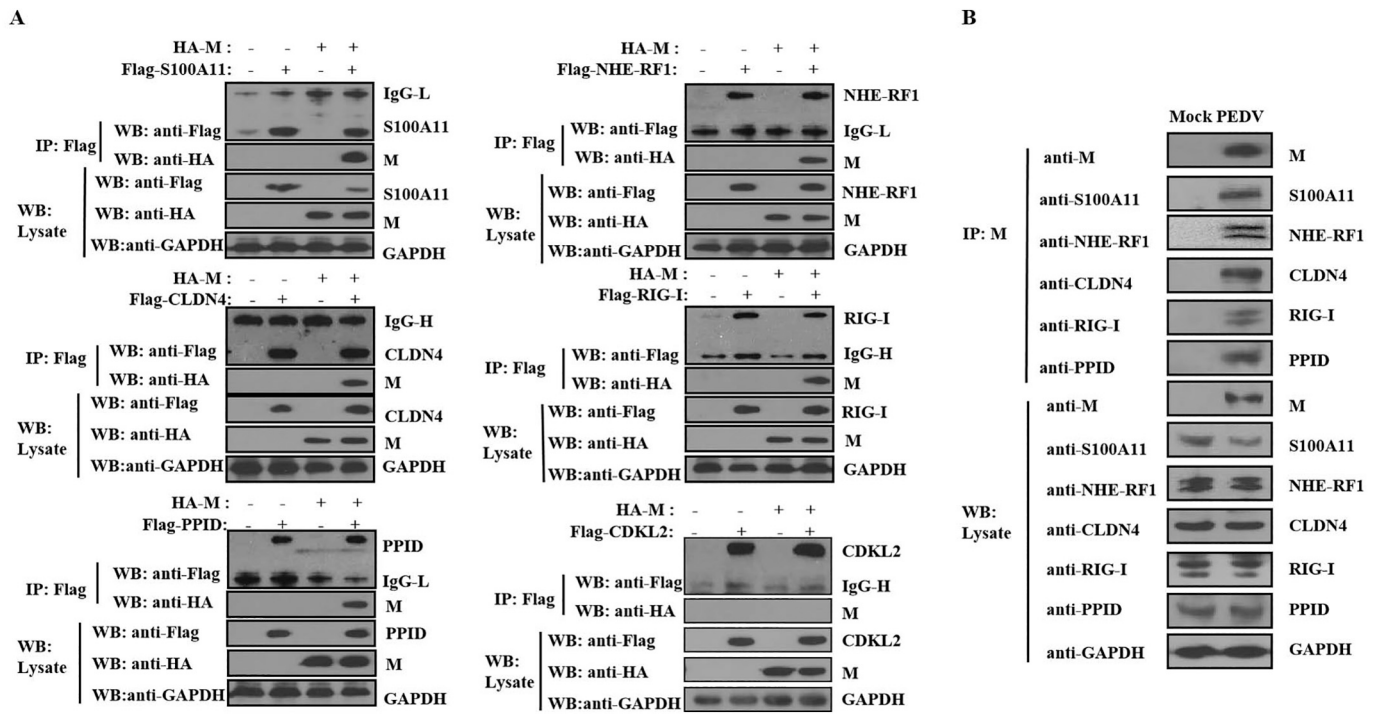


**Fig. 4.** Validation of interactions between PEDV M protein and host cell proteins with immunoblot analysis. (**A**) Immunoblot of M protein and host cell proteins precipitated using anti-Flag mAb from Hela cells co-transfected with pCAGGS-M-HA and pCAGGS-S100A11/NHE-RF1/CLDN4/RIG-I/PPID/ CDKL2-Flag. (**B**) Immunoblot analysis of precipitated proteins from mock- or PEDV-infected Vero cell lysates. Vero cells seeded in 10-cm-diameter culture dishes were infected with PEDV DR13$^{att}$ at a multiplicity of infection (MOI) of 0.1. After 36 h post-infection (hpi), the infected cells were lysed in RIPA lysis buffer. M protein and its interacting proteins were precipitated using anti-M-mAb and immunoblot analysis was carried out with anti-S100A11, -NHE-RF1, -CLDN4, -RIG-I, or -PPID polyclonal antibodies.

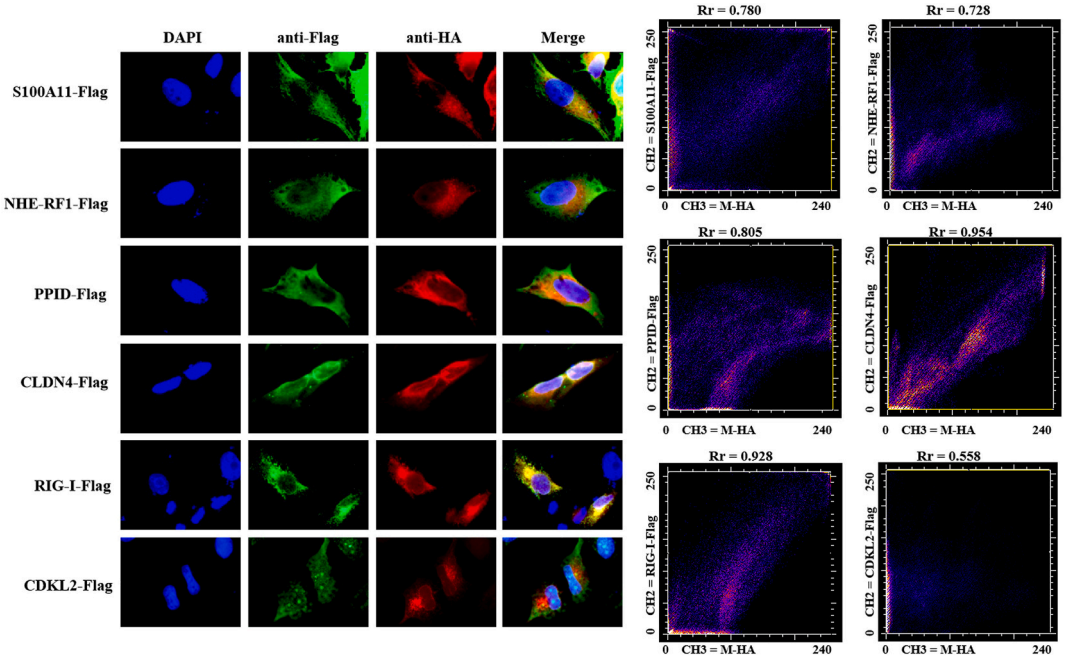


**Fig. 5.** Co-localization analysis of M protein with host cells proteins in Hela cells. Hela cells were co-transfected with plasmids expressing M-HA and S100A11/NHE-RF1/PPID/CLDN4/RIG-I/CDKL2-Flag proteins and the cells were fixed and stained with corresponding anti-HA and Flag mAb. The degrees of co-localization were assessed using the Pearson's correlation coefficient.

Silencing PPID had a protective effect against UVA-induced apoptosis in human keratinocytes [27], while our group reported that inhibition of cell apoptosis enhanced PEDV proliferation [9]. Thus, the increased PEDV replication observed when PPID expression is obstructed may be due to M protein interacting with PPID to block Vero cell apoptosis.

Proximity labeling has recently emerged as a new approach to detect transient and weak protein-protein interactions. APEX oxidizes phenol derivatives to phenoxyl radicals, which have a small labeling radius

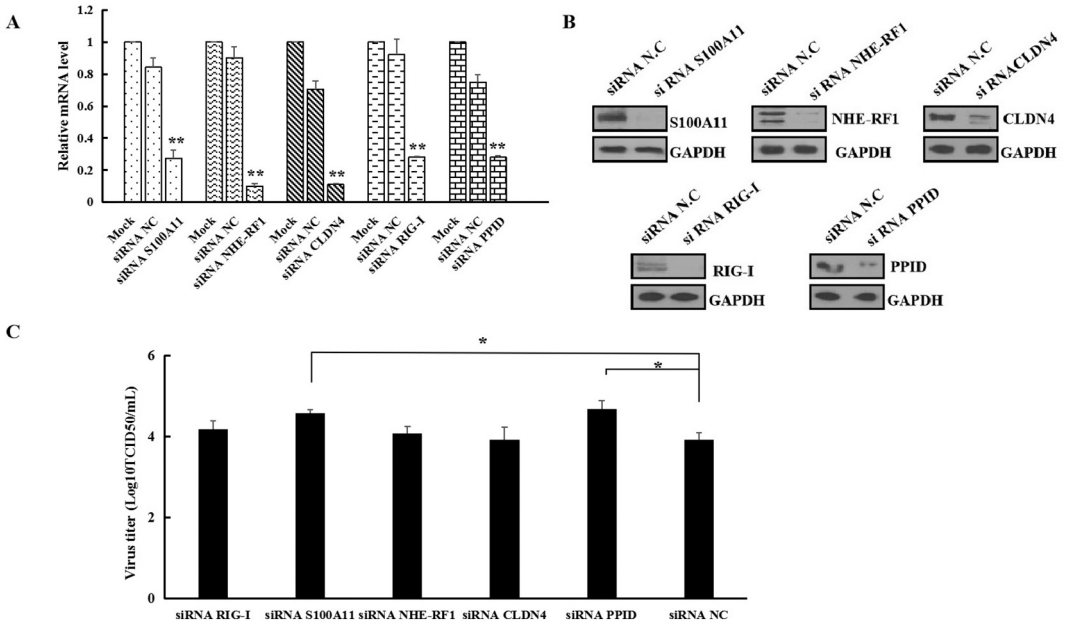


**Fig. 6.** Knockdown of five host cell proteins and the effects on PEDV production in Vero cells. (**A**) Relative mRNA levels of S100A11, NHE-RF1, CLDN4, RIG-I and PPID genes in cells transfected with control siRNA or the corresponding siRNAs determined by qRT-PCR. The data represent the means± SD for three independent experiments and were subjected to one-way ANOVA for statistical significance (** $p< 0.01$). (**B**) Relative protein expression levels of S100A11, NHE-RF1, CLDN4, RIG-I and PPID in cells transfected with siRNAs against S100A11, NHE-RF1, CLDN4, RIG-I, PPID, respectively and control siRNA determined by western blot. (**C**) Comparison of PEDV titers in cells transfected with siRNAs against S100A11, NHE-RF1, CLDN4, RIG-I, PPID and control siRNA. The data represent the means±SD for three independent experiments and were subjected to one-way ANOVA for statistical significance (*$p < 0.05$).

(<20 nm) [14]. APEX has been used to identify proteins within the human mitochondrial matrix [14], study proteomics of non-membrane-enclosed organelles [28] and identify novel receptors on the cell-surface [29]. In this study, we combined the APEX system with LC-MS/MS to successfully identify 40 intracellular proteins potentially capable of interacting with PEDV M. While there are shortcomings associated with the APEX system: e.g. trafficking deviation of studied proteins duo to increased molecular weights or structural changes (Fig. 1), these were overcome by validating the interacting proteins using the Co-IP test.

Our earlier research on M interacting proteins using Co-IP identified 218 proteins (Unique Peptide ≥1) [30], among which 21 proteins were coincident with the present study. Thus, most of the proteins identified by Co-IP and APEX2 labeling are different, making the two approaches complementary in terms of the data generated. Co-IP is a useful tool for detecting interacting proteins in the natural cellular environment but does not reveal proteins with transient or weak interactions [31]. APEX2 has a small labeling radius (<20 nm) and generates very short-lived radicals (<1 ms), that recognize proteins in close proximity to the target protein. Both methods are undoubtably valuable for uncovering the identity and scope of interacting proteins. Non-specificity is a feature of both methods, and it was for this reason that the different approaches were adopted in our study. Thus, co-localization and Co-IP analysis were used to verify the identified proteins. Non-specific values can be minimized by adopting appropriate controls and carrying out independent replicate determinations.

In conclusion, we have employed the proximity-labeling enzyme APEX2 to identify 40 host cell proteins that interact with PEDV M protein. Co-IP confirmed the interactions in the case of five of these proteins, two of which (PPID and S100A11) down-regulated viral replication. Our data provide new information relating to the novel functions of PEDV M protein.

## Data availability

The mass spectrometry proteomics data have been deposited with the ProteomeXchange Consortium (http://proteomecentral.proteomexchange.org) via the iProX partner repository with the dataset identifier PXD024559.


## Funding

This study was supported by the Shanghai Key Project on Agricultural Development (2020-02-08-00-12-F01478) and the Natural Science Foundation of China (31602060).


## CRediT authorship contribution statement

**Shijuan Dong:** Conceptualization, Methodology, Writing - original draft. **Ruiyang Wang:** Investigation. **Ruisong Yu:** Data curation. **Bingqing Chen:** Data curation. **Fusheng Si:** Resources, Software. **Chunfang Xie:** Resources, Software. **Zhen Li:** Supervision, Writing - review & editing.

## Declaration of Competing Interest

The authors declare that they have no competing interests.

## Data availability

Data will be made available on request.


## Acknowledgments

We thank Dr. Peter Rottier (Utrecht University) and Dr. Yao-Cheng Li (Salk Institute) for advice on the experiment design, Dr. Shaobo Xiao for the generous gift of anti-M monoclonal antibody and Dr. John Buswell for linguistic revision of the manuscript.


## Appendix A. Supplementary data

Supplementary data to this article can be found online at https://doi.org/10.1016/j.jprot.2021.104191.

## References


[1] E.N. Wood, An apparently new syndrome of porcine epidemic diarrhoea, Vet. Rec. 100 (1977) 243–244.

[2] J. Chen, X. Liu, D. Shi, H. Shi, X. Zhang, L. Feng, Complete genome sequence of a porcine epidemic diarrhea virus variant, J. Virol. 86 (2012) 3408.

[3] X.M. Wang, B.B. Niu, H. Yan, D.S. Gao, X. Yang, L. Chen, H.T. Chang, J. Zhao, C. Q. Wang, Genetic properties of endemic Chinese porcine epidemic diarrhea virus strains isolated since 2010, Arch. Virol. 158 (2013) 2487–2494.

[4] T. Oka, L.J. Saif, D. Marthaler, M.A. Esseili, T. Meulia, C. Lin, A.N. Vlasova, K. Jung, Y. Zhang, Q. Wang, Cell culture isolation and sequence analysis of genetically diverse US porcine epidemic diarrhea virus strains including a novel strain with a large deletion in the spike gene, Vet. Microbiol. 173 (2014) 258–269.

[5] G.W. Stevenson, H. Hoang, K.J. Schwartz, E.R. Burrough, D. Sun, D. Madson, V. L. Cooper, A. Pillatzki, P. Gauger, B.J. Schmitt, L.G. Koster, M.L. Killian, K.J. Yoon, Emergence of porcine epidemic diarrhea virus in the United States: clinical signs, lesions, and viral genomic sequences, J. Vet. Diagn. Investig. 25 (2013) 649–654.

[6] R. Kocherhans, A. Bridgen, M. Ackermann, K. Tobler, Completion of the porcine epidemic diarrhea coronavirus (PEDV) genome sequence, Virus Genes 23 (2001) 137–144.

[7] C. Li, Z. Li, Y. Zou, O. Wicht, F.J. van Kuppeveld, P.J. Rottier, B.J. Bosch, Manipulation of the porcine epidemic diarrhea virus genome using targeted RNA recombination, PLoS One 8 (2013), e69997.

[8] K. Wang, W. Lu, J. Chen, S. Xie, H. Shi, H. Hsu, W. Yu, K. Xu, C. Bian, W.B. Fischer, W. Schwarz, L. Feng, B. Sun, PEDV ORF3 encodes an ion channel protein and regulates virus production, FEBS Lett. 586 (2012) 384–391.

[9] F. Si, X. Hu, C. Wang, B. Chen, R. Wang, S. Dong, R. Yu, Z. Li, Porcine epidemic diarrhea virus (PEDV) ORF3 enhances viral proliferation by inhibiting apoptosis of infected cells, Viruses 12 (2020) 214–232.

[10] R.D. Woods, R.D. Wesley, P.A. Kapke, Neutralization of porcine transmissible gastroenteritis virus by complement-dependent monoclonal antibodies, Am. J. Vet. Res. 49 (1988) 300–304.

[11] Q. Zhang, K. Shi, D. Yoo, Suppression of typelinterferon production by porcine epidemic diarrhea virus and degradation of CREB-binding protein by nsp1, Virology 489 (2016) 252–268.

[12] X.G. Xu, H.L. Zhang, Q. Zhang, J. Dong, Y. Huang, D.W. Tong, Porcine epidemic diarrhea virus M protein blocks cell cycle progression at S-phase and its subcellular localization in the porcine intestinal epithelial cells, Acta Virol. 59 (2015) 265–275.

[13] K.J. Roux, D.I. Kim, M. Raida, B. Burke, A promiscuous biotin ligase fusion protein identifiifies proximal and interacting proteins in mammalian cells, J. Cell Biol. 196 (2012) 801–810.

[14] H.W. Rhee, P. Zou, N.D. Udeshi, J.D. Martell, V.K. Mootha, S.A. Carr, A.Y. Ting, Proteomic mapping of mitochondria in living cells via spatially restricted enzymatic tagging, Science 339 (2013) 1328–1331.

[15] S.S. Lam, J.D. Martell, K.J. Kamer, T.J. Deerinck, M.H. Ellisman, V.K. Mootha, A. Y. Ting, Directed evolution of APEX2 for electron microscopy and proximity labeling, Nat. Methods 12 (2015) 51–54.

[16] J. Andrejeva, K.S. Childs, D.F. Young, T.S. Carlos, N. Stock, S. Goodbourn, R. E. Randall, The V proteins of paramyxoviruses bind the IFN-inducible RNA helicase, mda-5, and inhibit its activation of the IFN-beta promoter, Proc. Natl. Acad. Sci. U. S. A. 101 (2004) 17264–17269.

[17] K.L. Siu, K.H. Kok, M.H. Ng, V.K. Poon, K.Y. Yuen, B.J. Zheng, D.Y. Jin, Severe acute respiratory syndrome coronavirus M protein inhibits type I interferon production by impeding the formation of TRAF3.TANK.TBK1/IKKε complex, J. Biol. Chem. 284 (2009) 16202–16209.

[18] K.L. Siu, C.P. Chan, K.H. Kok, P. Chiu-Yat Woo, D.Y. Jin, Suppression of innate antiviral response by severe acuterespiratory syndrome coronavirus M protein is mediated through the first transmembrane domain, Cell. Mol. Immunol. 11 (2014) 141–149.

[19] L. Cao, X. Ge, Y. Gao, G. Herrler, Y. Ren, X. Ren, G. Li, Porcine epidemic diarrhea virus inhibits dsRNA-induced interferon-β production in porcine intestinal epithelial cells by blockade of the RIG-I-mediated pathway, Virol. J. 12 (2015) 127.

[20] Q. Zhang, K. Shi, D. Yoo, Suppression of type I interferon production by porcine epidemic diarrhea virus and degradation of CREB-binding protein by nsp1, Virology 489 (2016) 252–268.

[21] M. Meng, L. Sang, X. Wang, S100 calcium binding protein A11 (S100A11) promotes the proliferation, migration and invasion of cervical cancer cells, and activates Wnt/ β-catenin signaling, Onco. Targets Ther. 12 (2019) 8675–8685.

[22] M. Sakaguchi, M. Miyazaki, Y. Inoue, T. Tsuji, H. Kouchi, T. Tanaka, H. Yamada, M. Namba, Relationship between contact inhibition and intranuclear S100C of normal human fibroblasts, J. Cell Biol. 149 (2000) 1193–1206.

[23] S. Pfefferle, J. Schopf, M. Kogl, C.C. Friedel, M.A. Muller, J. Carbajo-Lozoya, T. Stellberger, E. von Dall'Armi, P. Herzog, S. Kallies, D. Niemeyer, V. Ditt, T. Kuri, R. Zust, K. Pumpor, R. Hilgenfeld, F. Schwarz, R. Zimmer, I. Steffen, F. Weber, V. Thiel, G. Herrler, H. Thiel, C. Schwegmann-Wessels, S. Pohlmann, J. Haas, C. Drosten, B. Albreect, The SARS-coronavirus-host interactome: identification of cyclophilins as target for pan-coronacirus inhibitors, PLoS Pathog. 7 (2011), e1002331.

[24] W.B. Pratt, M.D. Galigniana, J.M. Harrell, D.B. DeFranco, Role of hsp90 and the hsp90-binding immunophilins in signaling protein movement, Cell. Signal. 16 (2004) 857–872.

[25] T. Ratajczak, B.K. Ward, R.F. Minchin, Immunophilin chaperones in steroid receptor signalling, Curr. Top. Med. Chem. 3 (2003) 1348–1357.

[26] P.D. Reynolds, Y.D. Ruan, F. Smith, J.G. Scammell, Glucocorticoid resistance in the squirrel monkey is associated with overexpression of the immunophilin FKBP51, J. Clin. Endocrinol. Metab. 84 (1999) 663–669.

[27] J. Jandova, J. Janda, J.E. Sligh, Cyclophilin 40 alters UVA-induced apoptosis and mitochondrial ROS generation in keratinocytes, Exp. Cell Res. 319 (2013) 750–760.

[28] D.U. Mick, R.B. Rodrigues, R.D. Leib, C.M. Adams, A.S. Chien, S.P. Gygi, M. V. Nachury, Proteomics of primary cilia by proximity labeling, Dev. Cell 35 (2015) 497–512.

[29] Y. Zhen, E.M. Haugsten, S.K. Singh, J. Wesche, Proximity labeling by a recombinant APEX2-FGF1 fusion protein reveals interaction of FGF1 with the proteoglycans CD44 and CSPG4, Biochemistry 57 (2018) 3807–3816.

[30] R. Wang, R. Yu, B. Chen, F. Si, J. Wang, C. Xie, C. Men, S. Dong, Z. Li, Identification of host cell proteins that interact with the M protein of porcine epidemic diarrhea virus, Vet. Microbiol. 246 (2020) 108729.

[31] S. Have, S. Boulon, Y. Ahmad, A.I. Lamond, Mass spectrometry-based immune-precipitation proteomics-the user's guide, Proteomics 11 (2011) 1153–1159.